

ENHANCING BRAIN CONNECTIVITY MAPPING: A RADIOMICS APPROACH TO DIFFUSION MRI TRACTOGRAPHY

LEVENTE ZSOLT NAGY

Thesis supervisor
ALFREDO VELLIDO ALCACENA (Department of Computer Science)

Thesis co-supervisor
ESTELA CAMARA MANCHA (Hospital Universitari de Bellvitge)

Degree
Master's Degree in Artificial Intelligence

Master's thesis

School of Engineering
Universitat Rovira i Virgili (URV)

Faculty of Mathematics
Universitat de Barcelona (UB)

Barcelona School of Informatics (FIB)
Universitat Politècnica de Catalunya (UPC) - BarcelonaTech

Abstract

This thesis about medical imaging aims to find alternative ways to map brain connectivity, utilizing the T1 and T2 MRI images instead of the diffusion MRI image, vastly improving the cost and time efficiency of the process. As a replacement for tractograpy, the currently used and accepted tool for processing the diffusion images, this thesis will reveal if there are any simple or complex relationship between radiomic features of the T1 and T2 images of the brain regarding the connected regions. The results and conclusions are limited to the connectivity of the basal ganglia to other main cortical regions of the brain. It is in no way a generalized conclusion, but rather a proof of concept from experiments ran on a specific dataset, provided by Hospital Universitari de Bellvitge.

Contents

List of Notations & Abbreviations

MRI magnetic resonance imaging 6

dMRI diffusion magnetic resonance imaging 6

FA fractional anisotropy 6

MD mean diffusivity 6

RD radial diffusivity 6

ROI region of interest 6

FNN feedforward neural network 16

NIfTI neuroimaging informatics technology initiative 9

FMRIB functional magnetic resonance imaging of the brain

FNIRT FMRIB's nonlinear image registration tool 6

GLCM gray level co-occurrence matrix 13

GLSZM gray level size zone matrix 13

GLRLM gray level run length matrix 13

NGTDM neighbouring gray tone difference matrix 13

GLDM gray level dependence matrix 13

List of Figures

List of Tables

Introduction

Basal ganglia is a part of the human brain which is group of subcortical nuclei responsible primarily for motor control, as well as other roles such as motor learning, executive functions and behaviors, and emotions. [1] Huntington's disease is a disorder that causes the progressive degeneration of the basal nuclei. [2]

Hospital de Bellvitge provided an excellent dataset of magnetic resonance imaging (MRI) and diffusion magnetic resonance imaging (dMRI) records of 32 control and 37 Huntington patient records of T1 and T1/T2 MRI images with isotropic voxels of 1 millimeter resolution and dMRI fractional anisotropy (FA), mean diffusivity (MD) and radial diffusivity (RD) images with isotropic voxels of 2 millimeter resolution and 1 second temporal resolution. Furthermore this dataset also contains the mask for the basal ganglia, which will also be referenced as the region of interest (ROI). And taking inspiration from this paper [3], masks for the 7 main cortical regions of the brain, which will also be referenced as the target regions: Limbic, Executive, Rostral-Motor, Caudal-Motor, Parietal, Occipital and Temporal are also included in the dataset. Tractography was performed on the dMRI images to figure out which parts of the ROI are connected to which cortical target, in a similar manner to how it was done in said paper [3]; where the relative connectivity maps are representing the ratio of the number of streamlines to each cortical target. Furthermore, the raw streamline images are also available, where there are a maximum of 5000 streamlines from each voxel in the ROI. The subcortical segmentation of the Basal Ganglia is also available, for the Caudate ,Putamen and Accumbens on the control patients. And lastly FMRIB's nonlinear image registration tool (FNIRT) warp fields were also provided for converting the records into normalized space.

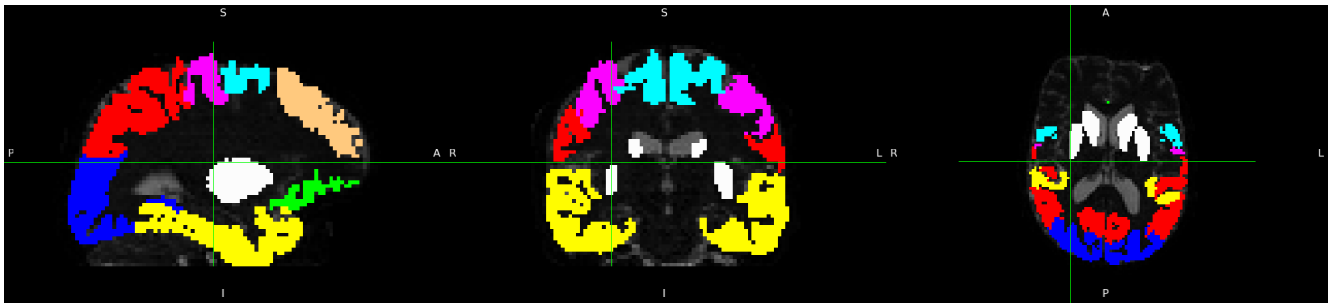

Figure 1.1: Basal Ganglia (ROI) & Cortical Targets

Color	Region
White	Basal Ganglia (ROI)
Green	Limbic
Brown	Executive
Light Blue	Rostral-Motor
Purple	Caudal-Motor
Red	Parietal
Blue	Occipital
Yellow	Temporal

Table 1.1: Regions Legend

Furthermore, for both the ROI and cortical targets, the dataset distinguishes between the right and left halves of the brain. Thus there are actually 2 ROIs and $2 \cdot 7 = 14$ target regions.

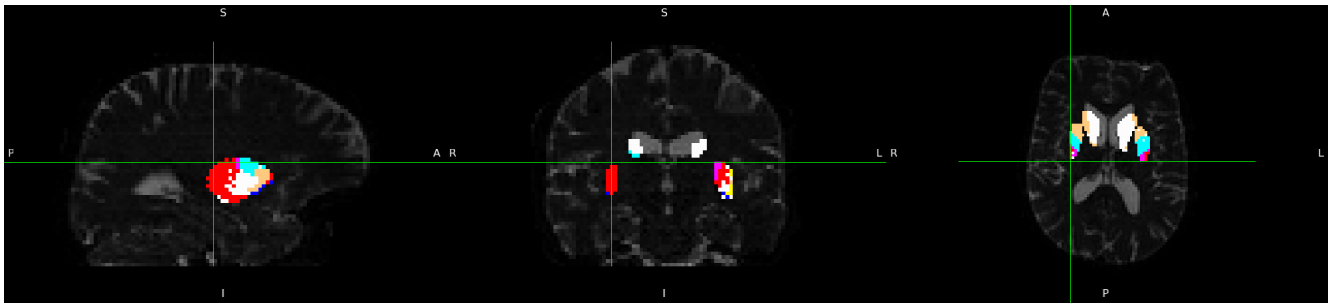

Figure 1.2: Connectivity Maps

1.1 Objectives

The end goal is to predict the relative connectivity of the Basal Ganglia to the cortical targets, from the radiomics features of the T1 and T1/T2 images.

This being a very complex problem, there is the possibility that the correlation between the connectivity of the brain and the T1, T1/T2 images are too weak to be mapped on this dataset. As from a datascience perspective, 69 datapoints are not much. But from a medical perspective it is substantial as it is very hard to collect uniform, clean data, with permissions to use it for research.

A simpler task leading up to the complex end goal, is a model for the simple segmentation of the Basal Ganglia for the regions Caudate Putamen and Accumbens. In order to confirm that the radiomics texture of the T1 and T1/T2 images of this dataset are are correlated to the anatomical segmentation of the Basal Ganglia. This problem is inherently connected to the main goal, as the relative connectivity does obey certain anatomical restrictions, and the anatomical segmentation of the Basal Ganglia is confirmed to be related to the relative connectivity. Thus if this simpler prediction fails, there is a good chance that the complex end goal will fail as well.

The biggest obstacle of this project is the preprocessing of the data, as there are many variations and hyperparameters that can be tuned. An exhaustive search definitely will not be viable, thus the preprocessing and model will needed to be tuned in a waterfall like manner, making educated guesses and comparing model performances across different tries. The main metric to measure

model performance, will be the accuracy of the label prediction across voxels, as it should be comparable between all approaches.

1.2 Motivation

The motivation for predicting the connectivity maps from the T1 and T1/T2 MRI images, is skipping the time and resource consuming process performing dMRI and tractorgrapy.

1.3 State of the Art

Design

2.1 Preprocessing

2.1.1 Raw Data

All provided data are in the neuroimaging informatics technology initiative (NIfTI) format, first these are need to be understood and parsed. This format stores the raw output of the MRI record, and additionally an affine transformation matrix used for aligning different spaces.

2.1.1.a Available Data

The following data will be preprocessed and read, even if not all of them are going to be used later on it helps providing the largest possible flexibility.

Data	**Shape**	**Range**	**Type**	**Space**	**Reference**
dMRI	(118, 118, 60, 74)	$[0, 4096]$	uint	diffusion	diffusion
Diffusion FA	(118, 118, 60)	$[0,\ 2]$	float	diffusion	diffusion_fa
Diffusion MD	(118, 118, 60)	$[0,\ 0.01]$	float	diffusion	diffusion_md
Diffusion RD	(118, 118, 60)	$[0,\ 0.01]$	float	diffusion	diffusion_rd
T1	(208, 256, 256)	$[0,\ 1000]$	float	t1	t1
T1/T2	(208, 256, 256)	$[0, 1]$	float	d_aligned	t1t2
Cortical Targets	(118, 118, 60, 14)	$\{0, 1\}$	bool	diffusion	targets
Relative Connectivity	(118, 118, 60, 14)	$[0, 1]$	float	diffusion	connectivity
Streamline Image	(118, 118, 60, 14)	$[0, 5000]$	uint	diffusion	streamline
ROI Mask (Basal Ganglia)	(118, 118, 60, 2)	$\{0, 1\}$	bool	diffusion	mask_basal & roi
Brain Mask	(208, 256, 256)	$\{0, 1\}$	bool	t1	mask_brain
Basal Ganglia Segmentation	(208, 256, 256)	$[0, 58]$	uint	t1	basal_seg

Table 2.1: Raw Datapoint

2.1.1.b Brain Mask

The provided dataset did not apply the brain masks for the T1 images out of the box so it can be done with a simple element wise multiplication of the T1 image and T1 mask.

2.1.1.c Registration

The process of aligning different records into the same native space is called "registration". The provided dataset comes with with 2 (3) different spaces, earlier referenced to as t1 and diffusion (and d_aligned). Most of the data are in diffusion space, thus it is logical to register the rest into

the same space. After manual inspection, only 15 datapoints required registration. Out of which 3 only required a tiny translation, and the rest 12 needed a complete affine registration.

The image T1/T2 is the odd one out, as it is inherently in a different space from diffusion (due to them being different resolution). But they are aligned into diffusion space. Although they do not need to be registered, this has to be taken into account later on.

2.1.1.d Normalization

The process of warping each brain into a common space is called "normalization". Applying the FNIRT warp fields are more or less straight forward, as two warp fields are provided, one for the diffusion space and one for the T1 space. Note that this process inherently contains the benefits of registration, as it is aligning the different images into a common space. This also paves the direction of future experiments, as it opens the door to working in either native and normalized space.

The only encountered obstacle was with the T1/T2 image. As it is aligned in diffusion space, but FNIRT convention ignores the affine transformation of the NIfTI format, thus making it's registration useless as the raw data of the t1t2 has nothing to do with the raw diffusion data (due to them being different resolution). The solution is to apply an affine matrix to t1t2's raw data which transforms it into t1's raw data space, after which the t1's FNIRT warp field can be applied to the t1t2 image. This affine transformation matrix can be easily calculated from the already given matrices. Let A denote T1/T2's affine matrix and B denote T1's affine matrix (after registration), thus the matrix which transforms the T1/T2 into T1 space is $M = A \cdot B^{-1}$.

2.1.1.e Basal Ganglia Segmentation

As the tractography of the brain is performed on the diffusion image, it inherently means that the connectivity maps and the roi are in diffusion space. But the basal ganglia's subcortical segmentation is in T1 space, which means that even if they are in the same space due to the different resolutions they will not have a pixel perfect union.

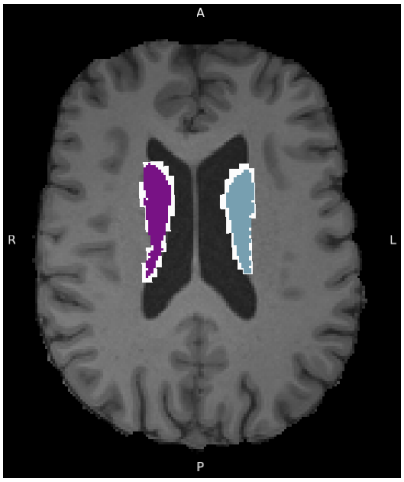

Figure 2.1: Basal Ganglia Subcortical Segmentation

The figure above visualizes the alignment of the Caudate subcortical region, where the white (larger) region is the Basal Ganglia mask from the diffusion space and the colored (smaller) regions are the Basal Ganglia segmentation from T1 space.

In order to keep the data consistent, mapping the segmentation to the Basal Ganglia mask can be done by assigning the same label for each voxel in the basal ganglia as the label of the closest voxel in the subcortical segmentation.

2.1.1.f N-Dim Array

The used NIfTI format stores the raw voxel space and the affine transformation matrix separately, in order to not loose data in the process of interpolating voxels when applying the transformation. But in order to consistently compare voxel data across different spaces (even if they are registered in the same space), the transformation needs to be applied, computing the interpolated voxels in the common space, bringing them into the same raw format of matching X, Y and Z dimensions, and discarding the stored affine matrices.

By default the native anatomical space's origin is near the center of mass of the brain, between the ears. The makes sense for medical professionals, when working with MRI records, but datastructure wise an array is indexed from 0. Meaning after applying the transformation to the voxel space, the yielded array will only contain one quadrant of the record as the rest are clipped in the negative regions. Thus the space is also needed to be translated with the negative vector of the transformed space's bounding box's lower end.

The translation value can be calculated by calculating the boundaries of the transformed space's bounding box. Get all 8 corners of the voxel space and apply the transformation matrix to all of them. Then get the min-max coordinates along X, Y and Z from the 8 transformed vectors, yielding the lower and upper bounds of the transformed space's bounding box.

It is very important to use the same translation value across different spaces to properly align them in the native space. For example let D and T denote a diffusion and t1 records and M_D and M_T denote their respective transformation matrices. Let T_D and T_T denote their respective translation values. In order to properly align them we need to apply $A_D = (M_D \cdot T_D)$ matrix and $A_T = (M_T \cdot T_D)$ matrix to D and T respectively, with matching T_D translation values.

The last issue is the missaligned length of the dimensions of the T1 and diffusion records. This can be simply fixed by truncating the excess along each dimension.

2.1.1.g Uniform Shape

After aligning the data into the same space per datapoint, it is still very likely that the individual datapoints do not have a uniform shape. This is due to them being in native space, some records will contain a smaller volume brain, some will contain a larger, they will not be the same.

Fixing this can be done by figuring out the min-max boundaries along each axis that the brain masks take up in the voxel space. Then the range of the masks along each axis can be calculated from the lower and upper boundaries per datapoint. And then the max range can be selected per axis, across all datapoints, yielding the new uniform shape. Finally, the voxel spaces can be sliced down to the new uniform shape, which can fit all brains of all data points (with some padding for most of them).

Note that this fix also greatly improves space efficiency, as it cuts out the unused voxels. This will be beneficial for storage and computational demands of future experiments.

Data	Volumes	Range	Type
diffusion	74	$[0, 4096]$	float16
diffusion_fa	1	$[0, 2]$	float16
diffusion_md	1	$[0, 0.01]$	float16
diffusion_rd	1	$[0, 0.01]$	float16
t1	1	$[0, 1000]$	float16
t1t1	1	$[0, 1]$	float16
targets	14	$\{0, 1\}$	bool
connectivity	14	$[0, 1]$	float16
streamline	14	$[0, 5000]$	float16
mask_basal	2	$\{0, 1\}$	bool
mask_brain	1	$\{0, 1\}$	bool
basal_seg	6	$\{0, 1\}$	bool

Table 2.2: Uniform Data

The uniform voxel space shapes are $(155, 199, 158)$ and $(147, 191, 155)$ for the native and normalized sets.

2.1.2 Quality Control

Having a low count of datapoints means that if there are even just a few outliers, it can heavily affect the end result. Thus all data were manually inspected to make sure they are clean as possible.

2.1.2.a Mismatched Data

Looking through the diffusion, diffusion_fa, diffusion_md and diffusion_rd images, 2 datapoints' FA, MD and RD images were seemingly from completely different patients. Thus the FA, MD and RD images were omitted for 2 datapoints.

2.1.2.b Garbled Data

Looking through the subcortical segmentation of the Basal Ganglia revealed that 1 datapoint had a garbled segmentation. Thus, said basal_seg image was omitted for 1 datapoint.

And one datapoint had a garbled T1 FNIRT warp field. Said datapoint was entirely omitted from the normalized set of datapoints.

2.1.2.c Missing Data

Looking through the relative connectivity and streamline images, 3 datapoints were missing these images, said 3 datapoints were completely omitted, as these datapoints are effectively missing the labels.

And the t1t2 images were missing for 10 datapoints, but these were not omitted as the t1 images were present for these datapoints, thus experiments only concerning the t1 can have a bit more available data.

2.1.3 Radiomics Features

Extracting the voxel based radiomic features has two main parameters to tune, the bin width and the kernel width.

The two approaches for binning are absolute discretization and relative discretization. Where in the prior one, a fixed bin width is chosen and in the latter one, a fixed number of bins are chosen and the bin width scales relatively according to the min-max voxel values. This study found that "The absolute discretization consistently provided statistically significantly more reproducible features than the relative discretization." [4] Relying on this information, the obvious choice to start with is the absolute discretization.

The bin width and the kernel width will be tuned in later experiments. And possibly features calculated with different setting will be concatenated and used simultaneously for better results. The used default values will be 25 and 5 for the bin and kernel widths respectively.

The following types of radiomic features will be used:

Feature Type	**Number of Features**
first order	18
gray level co-occurrence matrix (GLCM)	23
gray level size zone matrix (GLSZM)	16
gray level run length matrix (GLRLM)	16
neighbouring gray tone difference matrix (NGTDM)	5
gray level dependence matrix (GLDM)	14
3D shape	17

Table 2.3: Radiomic Feature Types

2.1.3.a Voxel Based

The following 92 features will be calculated voxel based:

First Order	**GLCM**	**GLSZM**
Energy	Autocorrelation	SmallAreaEmphasis
TotalEnergy	JointAverage	LargeAreaEmphasis
Entropy	ClusterProminence	GrayLevelNonUniformity
Minimum	ClusterShade	GrayLevelNonUniformityNormalized
10Percentile	ClusterTendency	SizeZoneNonUniformity
90Percentile	Contrast	SizeZoneNonUniformityNormalized
Maximum	Correlation	ZonePercentage
Mean	DifferenceAverage	GrayLevelVariance
Median	DifferenceEntropy	ZoneVariance
InterquartileRange	DifferenceVariance	ZoneEntropy
Range	JointEnergy	LowGrayLevelZoneEmphasis
MeanAbsoluteDeviation	JointEntropy	HighGrayLevelZoneEmphasis
RobustMeanAbsoluteDeviation	Imc1	SmallAreaLowGrayLevelEmphasis
RootMeanSquared	Imc2	SmallAreaHighGrayLevelEmphasis

Skewness	Idm	LargeAreaLowGrayLevelEmphasis
Kurtosis	MCC	LargeAreaHighGrayLevelEmphasis
Variance	Idmn	
Uniformity	Id	
	Idn	
	InverseVariance	
	MaximumProbability	
	SumEntropy	
	SumSquares	
GLRLM	**NGTDM**	**GLDM**
ShortRunEmphasis	Coarseness	SmallDependenceEmphasis
LongRunEmphasis	Contrast	LargeDependenceEmphasis
GrayLevelNonUniformity	Busyness	GrayLevelNonUniformity
GrayLevelNonUniformityNormalized	Complexity	DependenceNonUniformity
RunLengthNonUniformity	Strength	DependenceNonUniformityNormalized
RunLengthNonUniformityNormalized		GrayLevelVariance
RunPercentage		DependenceVariance
GrayLevelVariance		DependenceEntropy
RunVariance		LowGrayLevelEmphasis
RunEntropy		HighGrayLevelEmphasis
LowGrayLevelRunEmphasis		SmallDependenceLowGrayLevelEmphasis
HighGrayLevelRunEmphasis		SmallDependenceHighGrayLevelEmphasis
ShortRunLowGrayLevelEmphasis		LargeDependenceLowGrayLevelEmphasis
ShortRunHighGrayLevelEmphasis		LargeDependenceHighGrayLevelEmphasis
LongRunLowGrayLevelEmphasis		
LongRunHighGrayLevelEmphasis		

Table 2.4: Voxel Based Radiomic Features

2.1.3.b Non-Voxel Based

3D Shape
MeshVolume
VoxelVolume
SurfaceArea
SurfaceVolumeRatio
Sphericity
Maximum3DDiameter
Maximum2DDiameterSlice
Maximum2DDiameterColumn
Maximum2DDiameterRow
MajorAxisLength
MinorAxisLength
LeastAxisLength
Elongation
Flatness

Table 2.5: Shape Based Radiomic Features

Experiments

First the initial generic hyper parameters were established for all models, which can be shared between different architectures.

Parameter	Value
radiomics_brain_raw	(70, 106, 1)

Table 3.1: Generic Initial Hyperparameters

3.1 Classification FNN

First the starter hyper parameters were established for the classification feedforward neural network (FNN) models.

3.1.1 Simple 1

Sources of Information

[1] José L Lanciego, Natasha Luquin, and José Obeso. "Functional neuroanatomy of the basal ganglia". In: *Cold Spring Harbor perspectives in medicine* (2012). URL: https://doi.org/10.1101/cshperspect.a009621.

[2] Olivia C Matz and Muhammad Spocter. "The Effect of Huntington's Disease on the Basal Nuclei". In: *Cureus* (2022). URL: https://doi.org/10.7759/cureus.24473.

[3] Hyungyou Park et al. "Aberrant cortico-striatal white matter connectivity and associated subregional microstructure of the striatum in obsessive-compulsive disorder". In: *Molecular Psychiatry* (2022). URL: https://doi.org/10.1038/s41380-022-01588-6.

[4] Loïc Duron et al. "Gray-level discretization impacts reproducible MRI radiomics texture features". In: *PLoS One* (2019). URL: https://doi.org/10.1371/journal.pone.0213459.